Chapter 2. Cation-π interactions in ligand recognition by serotonergic ($5\text{-}HT_{3A}$) and nicotinic acetylcholine receptors

2.1 Introduction

Synaptic transmission is largely mediated by neurotransmitters and the receptors that bind them. At the core of this process is the selective recognition and binding of a small molecule by its protein host. Despite the pharmacological and clinical significance of compounds that modulate synaptic signaling, the chemical basis of neurotransmitter binding has been difficult to determine. High-resolution structural data on neuroreceptors with bound agonists are only just becoming available[1-5], and functional data are still needed to distinguish which agonist-receptor interactions are mechanistically significant.

Nearly all neurotransmitters contain a cationic center, and a common strategy for biological recognition of cations is the cation-π interaction, the stabilizing interaction between a cation and the negative electrostatic potential on the face of an aromatic ring.[6, 7] Earlier work in the Dougherty group introduced a technique for the *in situ* identification of cation-π binding sites.[8] This technique relies on nonsense suppression methodology for site-specific introduction of an unnatural amino acid into a functioning receptor expressed in a living cell.[9-12] In the first application of the technique, a series of fluorinated Trp derivatives was introduced at various positions in the binding region of the nicotinic acetylcholine receptor (nAChR). At Trp 149 of the α-subunit, the EC_{50} of ACh for receptor activation was strongly correlated to the degree of fluorination, providing a strong indication that ACh binds to the nAChR through a cation-π interaction with Trp α149. This assessment was subsequently confirmed in 2001 by the

crystallization of a soluble acetylcholine-binding protein (AChBP) from the snail, *Lymnaea helicalis*.[2] AChBP shares significant structural and sequence homology with the nAChR ligand-binding domain. (Figures 2.1 and 2.2) The crystal structure of AChBP revealed that the binding site is a box of aromatic residues, including the critical Trp α149. (Figure 2.1) Electron density corresponding to a molecule of HEPES was seen in this box with its ammonium center bound to Trp α149, as expected for a cation-π interaction.

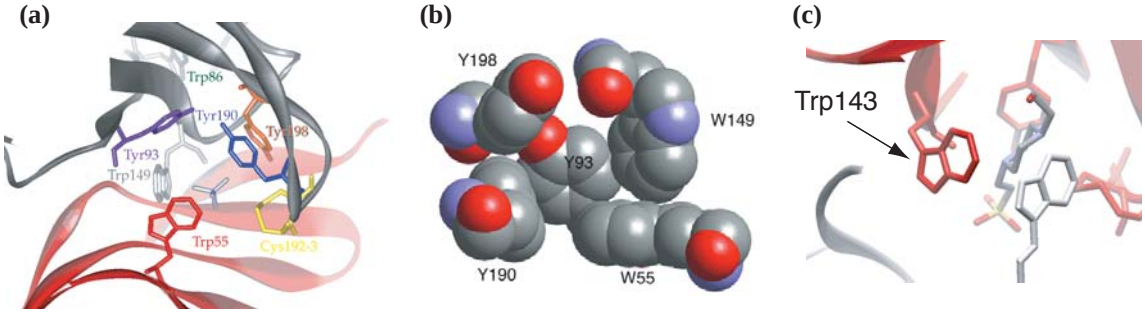

Figure 2.1. Several views of the nicotinic acetylcholine receptor (nAChR). (a) Details of the binding site illustrating the prevalence of aromatic residues. The coordinates come from X-ray diffraction of an ACh binding protein with high homology to nAChR. (b) The 'aromatic box' comprising the nAChR active site, based on AChBP coordinates. (c) Diffraction data from AChBP showing a HEPES molecule from the crystallization buffer bound to the face of Trp143, the homolog of muscle nAChR Trp149 and 5-HT_{3A}R Trp183.

In the work presented in this chapter, the F_n-Trp technique is utilized to examine the ligand-binding domain of the serotonin-gated ion channel, 5-HT_{3A}R. In addition, the cation-π interaction at the nAChR is further evaluated, considering nicotine and several other agonists. This work was done in collaboration with Gabriel Brandt who performed the majority of nAChR experiments. These studies generate two major findings. The first is that 5-HT_{3A}R Trp 183, which aligns with Trp α149 in the nAChR, binds the primary ammonium of serotonin (5-hydroxytryptamine, or 5-HT) via a cation–π

interaction. The second is that in the muscle nAChR, nicotine does not experience a strong cation-π interaction with Trp α149. The first result is consistent with the idea that the binding site of the serotonin channel is highly homologous to that of nAChR. The second result, however, is surprising in light of accepted pharmacophore models for the nicotinic receptor. Because of questions raised by these results, a series of both serotonin and nicotine derivatives were analyzed to better understand the role of the cation-π interaction in ligand recognition at these two receptors.

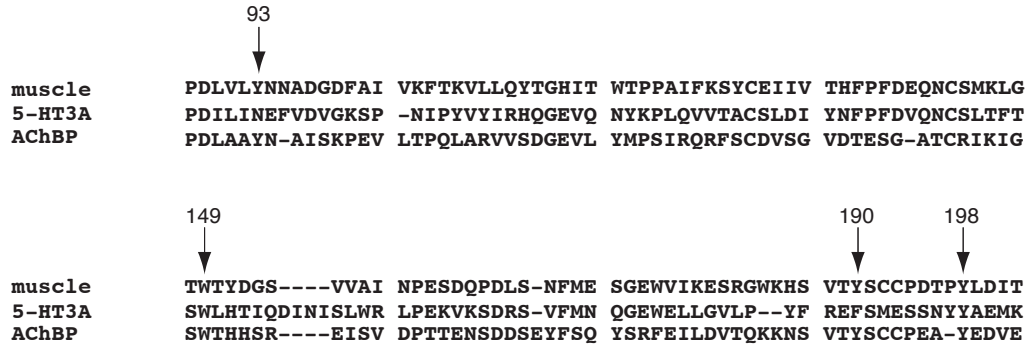

Figure 2.2. Sequence alignment of muscle nAChRα, 5-HT_{3A}R, and AChBP. The residues that comprise the aromatic box are indicated with arrows, with the exception of the Trp residue contributed by the interfacial subunit, which is conserved among all members of the nAChR receptor family and which is γ55 or δ57 in muscle nAChR and α90 in 5-HT_{3A}R.

2.2 Results

Unnatural amino acids were incorporated into the 5-HT_{3A}R and nAChR using *in vivo* nonsense suppression methods, and mutant receptors were evaluated electrophysiologically.[9-12] The structures and electrostatic potential surfaces of the side chains of the unnatural amino acids utilized are presented in Figure 2.3. Electrostatic potential surfaces provide a useful guide for evaluating the cation-π binding ability of an aromatic ring.[13, 14] These surfaces show how electron-withdrawing groups such as cyano

and fluoro substantially weaken the cation-π interaction. The agonists used in these studies are presented in Figure 2.4, along with their electrostatic potential surfaces. Note that the energy scales of the electrostatic potential plots are very different for Figures 2.3 and 2.4. For the side chains, the scale is ±25 kcal/mol, such that red is negative and blue is positive electrostatic potential. However, the structures of Figure 2.4 are all cations, and so the energy range is -5 to 160 kcal/mol. For a cation, the surface is positive everywhere; red simply represents relatively less positive, blue relatively more positive.

When studying weak agonists and/or receptors with diminished binding capability, we found it necessary to introduce a Leu to Ser mutation at a site known as 9' in the second transmembrane region of the receptor.[15, 16] This site is almost 50 Å from the binding site, and previous work has shown that each L9'S mutation lowers EC_{50} by a factor of roughly 10, with multiple L9'S mutations having an additive effect. Results from earlier studies and data reported below clearly demonstrate that trends in EC_{50} values are not perturbed by L9'S mutations[16]. For the present study, we used receptors that contain one or two L9'S mutations, as noted in the Tables and Figure captions.

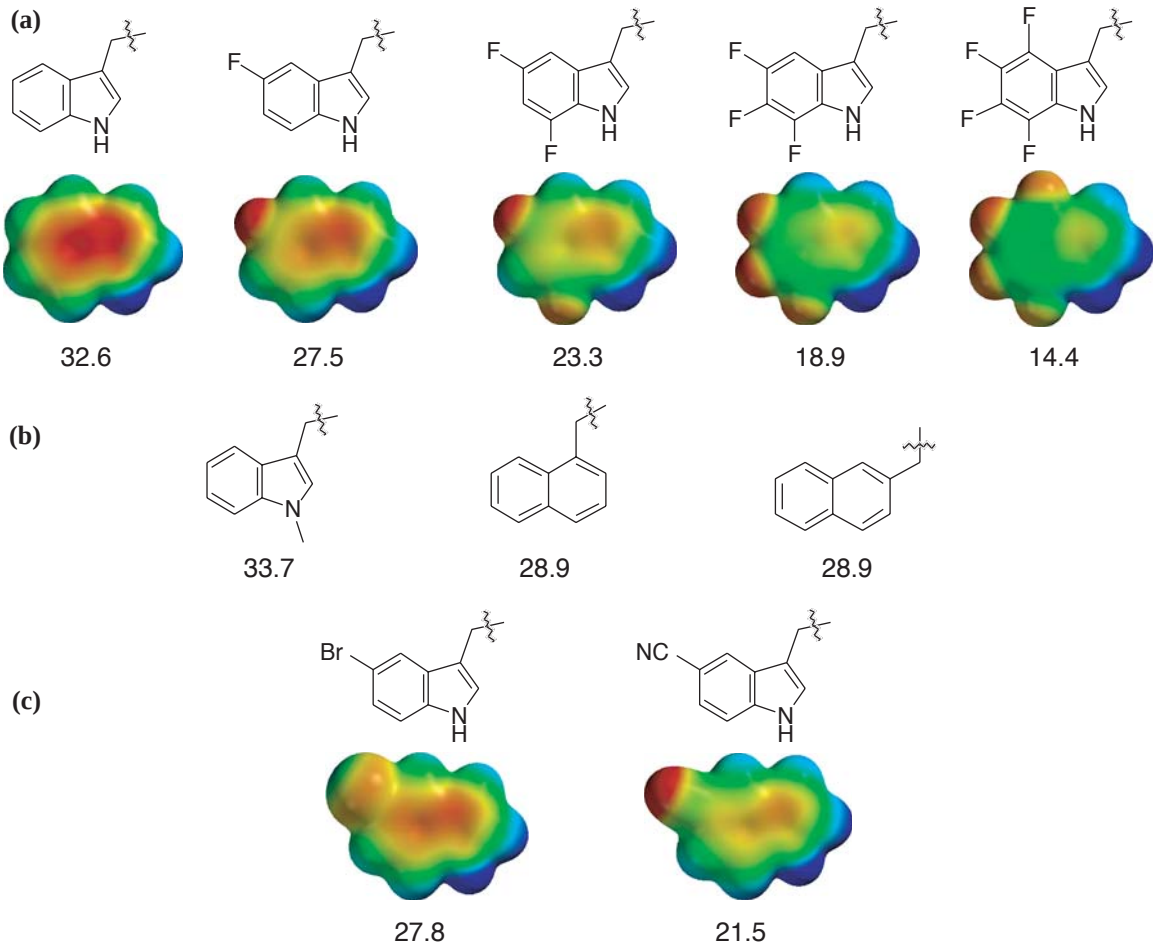

Figure 2.3. Side chains introduced in place of binding site Trp residues. (a) The series of fluorinated Trp analogs, with the gas-phase cation-π binding energy of fluoroindoles (HF 6-31G**) in kcal/mol. (b) Trp analogs without the indole nitrogen hydrogen bond donation ability, along with calculated cation-π binding energy. (c) Trp analogs for screening Trp sites for electrostatic interactions, with calculated cation-π binding ability. AM1 electrostatic surfaces are colored according to an energy scale corresponding to ±25 kcal/mol, where blue is positive and red negative.

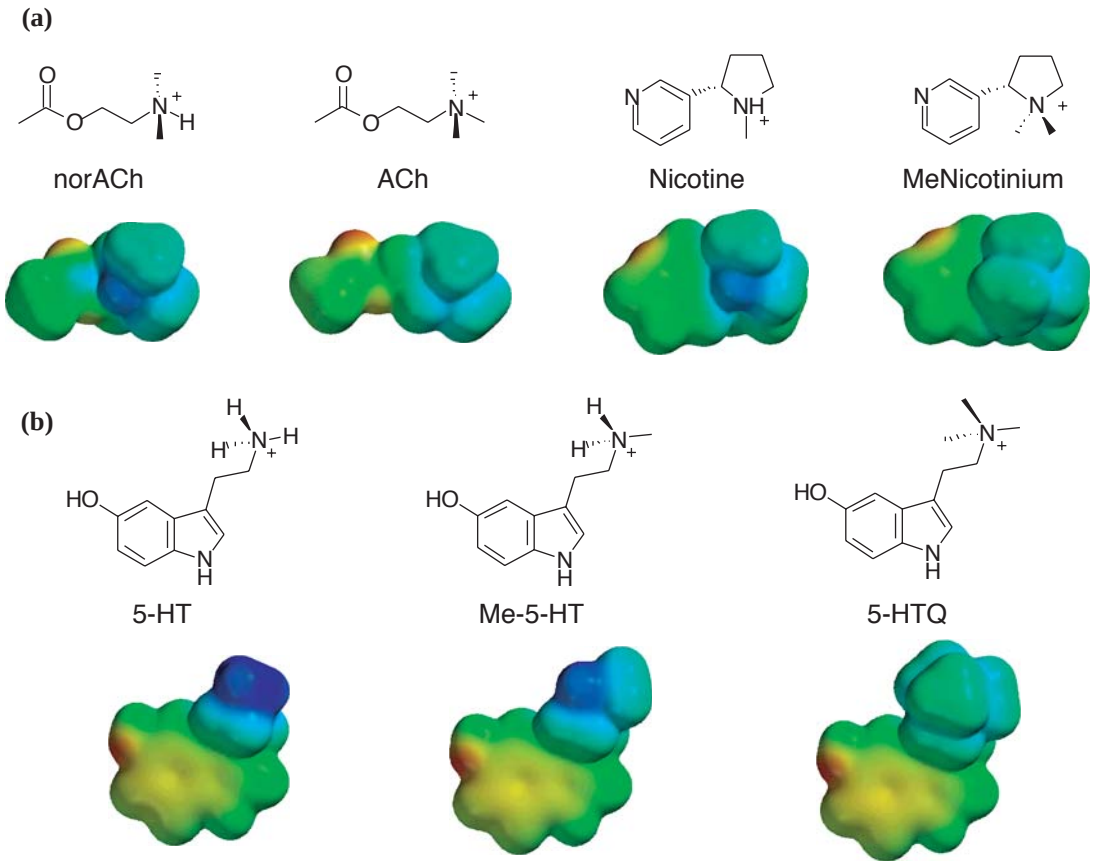

Figure 2.4. Agonists utilized in this study (a) nAChR agonists, with AM1 electrostatic surfaces calculated using Spartan showing the overall geometrical similarity of the structurally distinct nicotinoid and cholinergic agonists. (b) 5-HT_{3A}R agonists, with AM1 electrostatic surfaces showing the varying charge density around the nitrogen center. Electrostatic surfaces correspond to an energy range of –5 to +160 kcal/mol, where blue is positive and red negative.

Finally, it should be noted that the quantity reported here, EC_{50}, is not a binding constant, but a composite of equilibria for both binding and gating.[17] An advantage of EC_{50} is that it represents a *functional* assay; all mutant receptors reported here are fully functioning ligand-gated ion channels. This alleviates concerns that the mutations introduced cause a massive structural reorganization of the receptor. Because the subtle mutations we make are in the region of the agonist binding site, and the presumptive gate of the ion channel is almost 50 Å away, we assume variations in EC_{50} for the series of

unnatural residues reflect differential agonist-binding ability, and that the gating equilibrium is not substantially perturbed.

2.1.1 5-HT$_{3A}$R Studies

Two subunits, A and B, have been identified for the 5-HT$_3$R.[18, 19] Only the 5-HT$_{3A}$R when expressed alone in heterologous expression systems forms functional homomeric receptors, and the 5-HT$_3$R studies presented here were carried out using homomeric 5-HT$_{3A}$ receptors. Previous work has shown that the homomeric and heteromeric (A and B) receptors share a common pharmacology while differing somewhat in biophysical properties, such as conduction, kinetics, and desensitization characteristics.[20]

2.1.2 Position 183 in the 5-HT$_{3A}$R

Because of the well-established effect of fluorine substitution in modulating the cation-π interaction, a series of fluorinated Trp derivatives (5-F-Trp, 5,7-F$_2$-Trp, 5,6,7-F$_3$-Trp, and 4,5,6,7-F$_4$-Trp) was incorporated at position 183, the analog of Trp α149. Whole-cell currents and fits to the Hill equation, presented in Figure 2.5, demonstrate that these receptors display the functional hallmarks of 5-HT$_3$R's – desensitization to prolonged agonist exposure and Hill coefficients around two. The EC$_{50}$ values for the wild type and the mutants are given in Table 2.1. A clear trend can be seen from the data. Each additional fluorine produces an increase in EC$_{50}$. Re-introduction of the wild type residue, Trp, yielded an EC$_{50}$ of 1.21 μM, comparable to that obtained from the wild type receptor heterologously expressed in oocytes. If a single fluorine is added to the tryptophan ring EC$_{50}$ increases 5-fold to 6.03 μM. Addition of another fluorine to the

ring leads to a 31-fold increase (relative to wild type) in EC_{50}, 37.7 μM, and a third fluorine yields an EC_{50} of 244 μM, 201-fold greater than Trp.

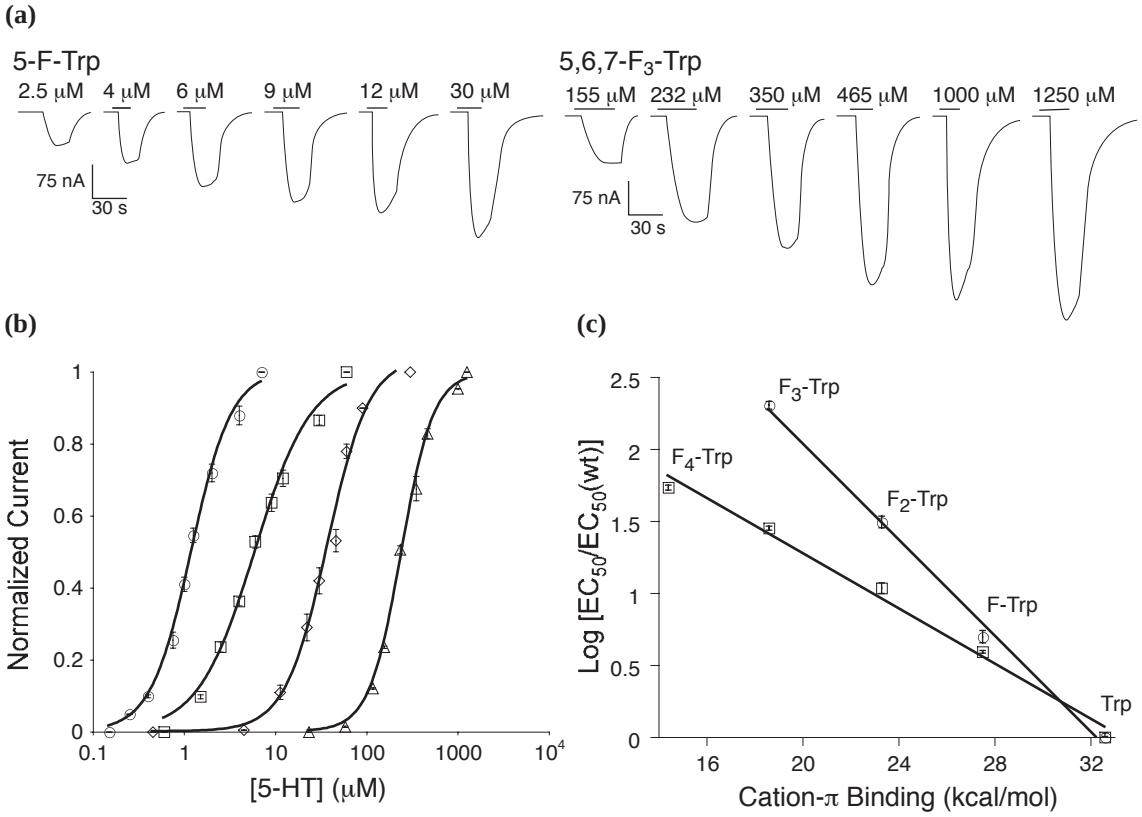

Figure 2.5. Electrophysiological analysis of 5-HT. (a) Representative voltage-clamp current traces for oocytes expressing suppressed 5-HT_{3A}R. Bars represent application of 5-HT. (b) 5-HT dose-response relations and fits to the Hill equation for 5-HT_{3A}R suppressed with Trp (*circles*), F–Trp (*squares*), F_2-Trp (*diamonds*), and F_3-Trp (*triangles*) at position 183. (c) Fluorination plot (log [EC_{50}/EC_{50} (wt)] versus calculated cation-π binding ability for the series of fluorinated Trp derivatives) for 5-HT (*circle*) at the 5-HT_{3A}R and ACh (*squares*) at the nAChR. 5-HT data fit the line y = 5.37 - 0.17x and ACh data fit the line y = 3.2 - 0.096x. The correlation for both linear fits is r = 0.99.

Attempts to record dose-response relations from the incorporation of 4,5,6,7-F_4-Trp at 183 were unsuccessful because this mutant required highly elevated concentrations of 5-HT— concentrations at which the agonist becomes an effective open channel-blocker. In a similar strategy to that used for the nAChR, a Val to Ser mutation was

introduced at position 13' in the M2 domain. This mutation has been shown to increase the agonist sensitivity of the 5-HT_3R.[21, 22] The EC_{50} values for the F_n-Trp series did show a progressive increase correlating with fluorination of the tryptophan ring, but did not entirely replicate the trend seen for receptors lacking this mutation (Table 2.1). Further analysis demonstrated that this mutation leads to standing currents that are reversible by addition of the open-channel blocker TMB-8, indicating this mutation produces constitutive activation of the receptor in the absence of agonist. For this reason, studies with the V13'S mutation were abandoned.

As in previous work on the nAChR, our measure for the cation-π binding ability of the fluorinated Trp derivatives is the calculated binding energy (kcal/mol) of a generic probe cation (Na^+) to the corresponding substituted indole.[8, 13] This provides a convenient way to express the clear trend in the dose-response data in a more quantitative way. Extensive studies of the cation-π interaction establish that *trends* in cation-π binding ability across a series of aromatics are independent of the identity of the cation, justifying the use of a simple probe ion. In order to also place the dose-response data for the channel on an energy scale, the logarithmic ratio of EC_{50} for mutants to EC_{50} for wild type is used. We refer to such representations as fluorination plots. A plot of this ratio versus cation-π binding ability for Trp183 reveals a compelling relationship (Figure 2.5c). Over a range of greater than two orders of magnitude in EC_{50}, there is a linear correlation between log (EC_{50}) and the cation-π binding ability of the side chains. This provides substantial evidence that Trp 183 binds 5-HT through a cation-π interaction arising from van der Waals contact between the agonist ammonium group and the indole side chain.

Table 2.1 Dose-response data for 5–HT_{3A}R and unnatural amino acids

	Residue	EC_{50}±SEM (μM)	Hill±SEM
	W183		
5-HT	Trp	1.21 ± 0.06	2.0 ± 0.16
	F-Trp	6.03 ± 0.5	1.4 ± 0.14
	F_2-Trp	37.7 ± 2.96	1.9 ± 0.23
	F_3-Trp	244 ± 8.4	2.5 ± 0.17
5-HT	Trp	0.04 ± 0.002	1.6 ± 0.06
V13'S	F-Trp	0.06 ± 0.003	1.8 ± 0.14
	F_2-Trp	0.27 ± 0.006	2.6 ± 0.13
	F_3-Trp	3.53 ± 0.141	2.2 ± 0.16
N-Me-5-HT	Trp	1.82 ± 0.10	2.5 ± 0.13
	F-Trp	2.70 ± 0.17	1.9 ± 0.19
	F_2-Trp	23.1 ± 2.73	2.6 ± 0.22
	F_3-Trp	368 ± 12	2.0 ± 0.10
5-HTQ	Trp	1.07 ± 0.07	2.1 ± 0.25
	F-Trp	1.65 ± 0.15	1.6 ± 0.19
	F_2-Trp	12.8 ± 0.95	1.8 ± 0.19
	F_3-Trp	284 ± 18.7	2.0 ± 0.15
5-HT	1-Np-Ala	30.4 ± 1.75	1.6 ± 0.10
	2-Np-Ala	32.0 ± 2.30	1.6 ± 0.12
	N-Me-Trp	25.6 ± 1.66	1.8 ± 0.16
	W90		
5-HT	Trp	1.21 ± 0.06	2.0 ± 0.16
	F_4-Trp	1.01 ± 0.05	1.6 ± 0.09

Along with modulating the cation-π interaction, fluorination also increases the ability of a Trp analog to donate a hydrogen bond.[23, 24] Therefore, an alternative interpretation of the above results would be that the hydrogen-bonding ability of the NH of the indole side chain of Trp 183 decreases receptor activation, and that fluorinated Trp analogs decrease activation by increasing the hydrogen-bond strength. This hypothesis suggests that EC_{50} would be decreased by side chains that remove the hydrogen bond, but

remain isosteric with Trp. To test this hypothesis, a series of Trp analogs lacking a hydrogen-bond donor at the nitrogen position of the indole was incorporated at position 183 (Figure 2.3b). The EC_{50} values for 2-Np-Ala, 1-Np-Ala, and N-Me-Trp were 32 μM, 30 μM, and 26 μM, respectively (Table 2.1). The increased EC_{50} is opposite to the prediction of the hydrogen-bond hypothesis. Thus, it appears that modulation of hydrogen-bonding ability does not explain the increase in EC_{50} in response to fluorination.

2.1.3 Position 90 in the 5-HT$_{3A}$R

An important question is whether the dramatic fluorination effect seen at position 183 in the 5-HT_{3A}R is unique to this site, as was observed for Trp α149 in the nAChR. In principle, the cation could interact simultaneously with several sides of the aromatic box. Based on sequence alignment and the AChBP structure, Trp 90— which aligns with Trp γ55/δ57— forms part of the binding site in the 5-HT_{3A}R. Thus, 4,5,6,7-F_4-Trp was incorporated at position 90. The EC_{50} value of this mutant was almost identical to wild type, 1.1 μM and 1.2 μM respectively, indicating that Trp 183 uniquely defines the cation-π binding site in the 5-HT_{3A}R (Table 2.1).

2.1.4 N-Me-5-HT and 5-HTQ at the 5-HT$_{3A}$R

Comparison of the fluorination plots for ACh and 5-HT shows that the slopes of the lines are quite different for the two agonists. The steeper slope seen for 5-HT indicates its ammonium center is more sensitive to electrostatic attenuation of the face of the tryptophan ring. Given the strong electrostatic component of the cation-π interaction, it is very likely this difference arises from the differing charge distributions between a

primary ammonium (5-HT) and a quaternary ammonium (ACh). To investigate this relationship further, we attempted to serially modulate the strength of the cation-π interaction by varying the degree of alkylation at the ammonium center.

Dose-response relations were recorded for the secondary serotonin analog, N-methyl-5-hydroxytryptamine (N-Me-5-HT) and the quaternary derivative, N,N,N-trimethyl-5-hydroxytryptamine (5-HTQ) with the fluoro-Trp series at position 183 (Figure 2.4b). The results for these experiments are presented in Table 2.1. Mono or tris methylation at the ammonium center of 5-HT has a minimal effect on EC_{50}; both agonists are comparable to the natural ligand, serotonin. At position 183 in the 5-HT_{3A}R— as with 5-HT itself— each additional fluorine substituent produces an increase in EC_{50}, indicating a significant cation-π interaction with the ammonium centers in both N-Me-5-HT and 5-HTQ (Figure 2.6).

Surprisingly, the expected trend for the substituted agonists (primary more sensitive than secondary, and secondary more sensitive than quaternary) is not seen. It is difficult to interpret these results, however, because in essence, these are double mutant studies with both the receptor and the agonist being simultaneously altered. It may be that though all three are potent agonists and bind to Trp 183 via a cation-π interaction, the binding mode for each is subtly different. Thus, the fluorination plots may be reporting on small differences in the binding distance and geometry between the ammonium center and aromatic face of the indole ring.

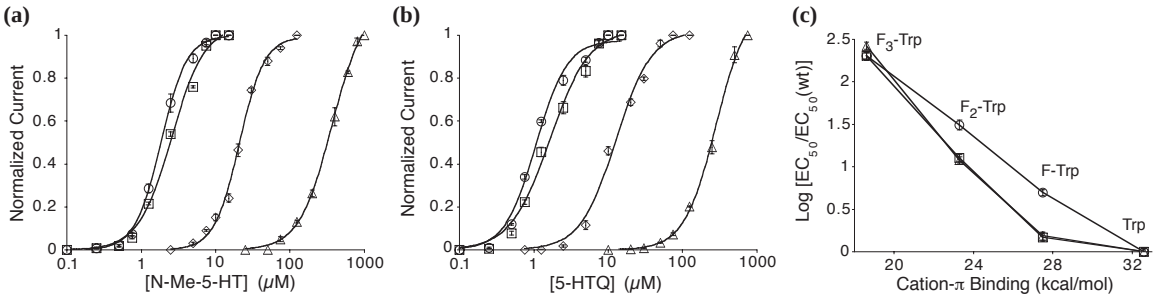

Figure 2.6. Electrophysiological analysis of 5-HT analogs. (a) N-Me-5-HT dose-response relations and fits to the Hill equation for 5-HT_{3A}R suppressed with Trp (*circles*), F–Trp (*squares*), F_2-Trp (*diamonds*), and F_3-Trp (*triangles*) at position 183. (b) 5-HTQ dose-response relations and fits to the Hill equation for 5-HT_{3A}R suppressed with Trp (*circles*), F–Trp (*squares*), F_2-Trp (*diamonds*), and F_3-Trp (*triangles*) at position 183 (c) Fluorination plot for 5-HT (*circles*) and N-Me-5-HT (*squares*) and 5-HTQ (*triangles*).

2.1.5 Effect of agonist alkylation state at the nAChR

As a complement to the studies of N-Me-5-HT and 5-HTQ at the 5-HT_{3A}R, Gabriel Brandt studied the behavior of the tertiary ACh analog, 2-dimethylaminoethyl acetate (noracetylcholine, or norACh) and the "simplified" quaternary ACh analog, tetramethylammonium (TMA) at the nAChR (Figure 2.4a). While TMA is a very low-potency agonist (Table 2.2), it does appear to experience a cation-π interaction with Trp α149 similar to that seen for ACh (Figure 2.7). Only data up to F_3-Trp are available because, as with other agonists studied, channel blockade by the agonist becomes a serious problem at the high concentrations necessary to activate the receptor with F_4-Trp at α149. However, it is clear that progressive fluorination leads to a steady increase in EC_{50} as seen with ACh.

The results for norACh highlight a significant difference between the 5-HT_{3A}R and the nAChR. While substantial variation in the alkylation state of 5-HT has no

significant effect on potency, simply removing one methyl group from the quaternary ammonium of ACh to produce norACh leads to vastly inferior potency. The EC_{50} for norACh is comparable to that of TMA. The fluorination data for norACh are not completely straightforward (Table 2.2). While monofluorination shows a 7-fold increase— comparable to ACh— di- and trifluorination show only modest increases and tetrafluorination leads to a *decrease* in EC_{50} (Figure 2.7).

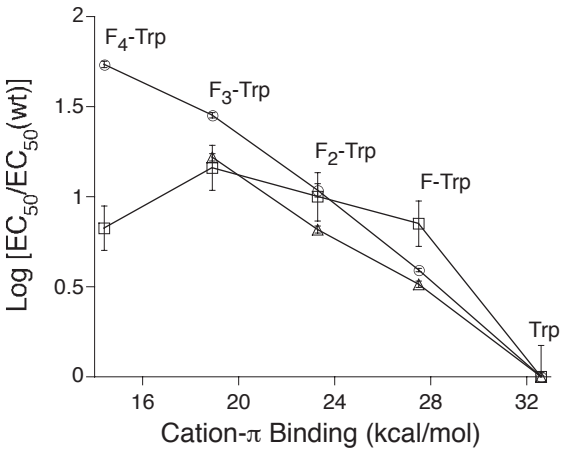

Figure 2.7. Fluorination plot for ACh (*circles*) and norACh (*squares*) and TMA (*triangles*).

2.1.6 Nicotine dose-response to F_n-Trp series at α149 in muscle nAChR

Nicotine is, of course, an important agonist of the nAChR, and all pharmacophore models for this drug and related compounds align the protonated pyrrolidine nitrogen with the quaternary ammonium of ACh.[25-29] To evaluate this model, we studied nicotine's potency with the series of fluorinated Trp derivatives at position α149 of the nAChR. The results are shown in Table 2.2 and Figure 2.8. Dose-response relations were collected for receptors with one (β subunit) or two (βγ subunits) L9'S mutations. The data for βL9'S receptors comes from Wenge Zhong, and Gabriel Brandt collected the

βγL9'S data. The results are similar in each case. If a single fluorine is added to the tryptophan ring by incorporating F-Trp at position α149, the EC_{50} increases almost three-fold, which is comparable to the four-fold increase observed with ACh. However, further fluorination does not lead to a significant further increase in EC_{50}. Figure 2.8c shows a fluorination plot for nAChR with a single L9'S mutation in the β subunit. Clearly, the progressive rise in EC_{50} seen with ACh and other agonists is not seen with nicotine.

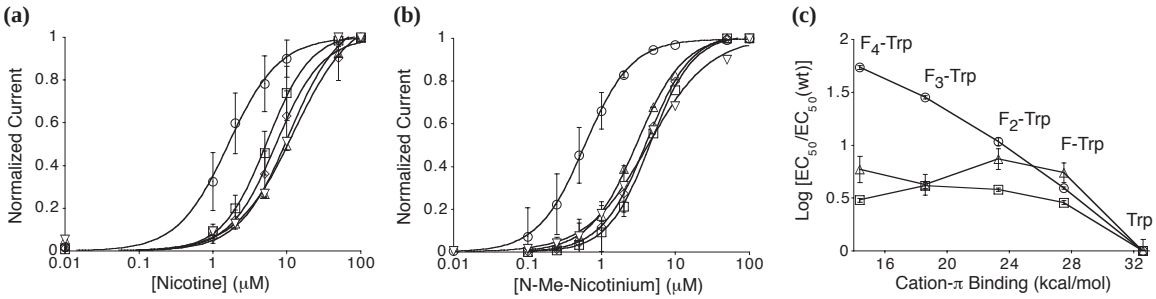

Figure 2.8. Electrophysiological analysis of nicotine and N-Me-nicotinium. (a) Nicotine dose-response relations and fits to the Hill equation for nAChR suppressed with Trp (*circles*), F–Trp (*squares*), F_2-Trp (*diamonds*), and F_3-Trp (*triangles*) at position 183. (b) N-Me-nicotinium dose-response relations and fits to the Hill equation for nAChR suppressed with Trp (*circles*), F–Trp (*squares*), F_2-Trp (*diamonds*), and F_3-Trp (*triangles*) at position 183 (c) Fluorination plot for ACh (*circles*) and nicotine (*squares*) and N-Me-nicotinium (*triangles*).

2.1.7 Nicotine dose-response to Trp analogs at γ55/δ57 in muscle nAChR

The lack of a strong response to fluorination at Trp α149 by nicotine indicates that it does not experience a significant cation-π interaction with this residue. This suggests the possibility that another aromatic residue in the binding site might form a cation-π interaction with nicotine. Based on the crystal structure of AChBP, an appealing candidate is Trp γ55/δ57, which is adjacent to Trp α149 in the binding site. We therefore evaluated the γ55/δ57 pair using, instead of fluorination, the alternative comparison of 5-CN-Trp vs. 5-Br-Trp. This nearly isosteric pair provides a useful qualitative indicator

of a cation-π interaction, since the cyano group is much more strongly deactivating than the bromo (Figure 2.3c). For example, at α149 with ACh as the agonist, the ratio of EC_{50} values for 5-CN-Trp/5-Br-Trp is 57.[8] As shown in Table 2.2, the ratio, 5-CN-Trp/5-Br-Trp is approximately 0.5 for nicotine at the γ55/δ57 position. This is not at all consistent with a cation-π interaction between nicotine and this tryptophan.

2.1.8 N-methyl-nicotinium dose-response to F_n-Trp series at nAChR α149

Both ACh and TMA show a progressive increase in EC_{50} with fluorination while nicotine does not. This suggests that a quaternary ammonium ion may be essential to see this effect in nAChR binding. To test this possibility, Gabriel Brandt evaluated the quaternary analog, N-methyl-nicotinium in the βγ L9'S nAChR. As shown in Table 2.2, the EC_{50} for N-methyl-nicotinium at wild-type receptors is similar to that of nicotine. In addition, N-methyl-nicotinium behaves quite similarly to nicotine in the fluorination plot. Thus, the unusual behavior of nicotine is not due to the lack of a quaternary ammonium group (Figure 2.8).

Table 2.2. Dose-response data for nAChR and unnatural amino acids

	Residue	EC_{50}±SEM (μM)	Hill±SEM
	W149		
Ach[a]	Trp	1.2 ± 0.0	ND[b]
β L9'S	F-Trp	4.7 ± 0.1	ND
	F_2-Trp	13 ± 1	ND
	F_3-Trp	34 ± 1	ND
	F_4-Trp	65 ± 3	ND
TMA	Trp	48 ± 2	ND
β,δ L9'S	F-Trp	155 ± 4	ND
	F_2-Trp	313 ± 8	ND
	F_3-Trp	789 ± 23	ND
norACh	Trp	23 ± 6	2.62 ± 1.00
β,γ L9'S	F-Trp	161 ± 9	1.92 ± 0.26
	F_2-Trp	225 ± 28	1.62 ± 0.04
	F_3-Trp	327 ± 18	1.62 ± 0.03
	F_4-Trp	152 ± 4	1.53 ± 0.03
Nicotine	Trp	45 ± 1	ND
β L9'S	F-Trp	130 ± 5	ND
	F_2-Trp	172 ± 6	ND
	F_3-Trp	188 ± 11	ND
	F_4-Trp	136 ± 5	ND
Nicotine	Trp	1.3 ± 0.3	2.92 ± 1.47
β,γ L9'S	F-Trp	4.2 ± 0.7	1.57 ± 0.09
	F_2-Trp	5.4 ± 0.5	1.53 ± 0.08
	F_3-Trp	12 ± 1	1.13 ± 0.07
	F_4-Trp	11 ± 1	1.28 ± 0.07
MeNicotinium	Trp	0.8 ± 0.1	1.34 ± 0.07
β,γ L9'S	F-Trp	4.2 ± 0.4	1.44 ± 0.08
	F_2-Trp	5.7 ± 0.7	1.42 ± 0.09
	F_3-Trp	3.3 ± 0.4	1.33 ± 0.07
	F_4-Trp	4.6 ± 1.0	1.05 ± 0.13
	Wγ55/δ57		
Nico	CN-Trp	1.4 ± 0.2	ND
α_2 L9'S	Br-Trp	3.0 ± 0.4	ND

[a] data from reference #7, Zhong et al. ,*PNAS* **1998**, 95, 12088.
[b] ND = no data

2.1.9 Studies of agonist efficacy

The EC_{50} for a receptor is a composite measurement comprising multiple elementary steps. Even in the simplest two-state model of channel opening, agonist binding to the closed channel is followed by a conformational change to an open channel state. Since the dose-response measurement does not distinguish between these two steps, experiments were undertaken to determine whether binding or channel gating accounted for the observed alterations in EC_{50} in response to increasing Trp fluorination. The efficacy of a compound on a ligand-gated ion channel is reflected in the maximal current passed at saturating agonist concentration under given electrophysiological conditions.[17, 30] Relative efficacies of all drugs were determined in ND96 medium in oocytes clamped at a membrane potential of -80 mV at a concentration five times the EC_{50} of the compound, and were determined for the various agonists at α149 suppressed receptors in nAChR and 183 suppressed receptors in 5-HT_{3A}R. The relative efficacy of each agonist was calculated as the ratio of I_{max} for the agonist to I_{max} for ACh or 5-HT.

For the 5-HT_3R and nAChR agonists considered here, there were no large statistical differences in efficacy among them (Table 2.3), nor was the relative efficacy ever observed to differ in receptors containing fluorinated Trp analogs. The process of channel gating is a complicated one and is postulated to involve numerous elementary steps for the nAChR. Thus, it is overly simplistic to conclude from these efficacy experiments that the effects observed are due exclusively to binding.[31] However, the fact that all compounds tested exhibit similar ability to initiate the conformational changes

associated with channel opening suggests the large effects that we see on potency most likely arise from effects on agonist binding.

Table 2.3 Efficacy values for the 5–HT_{3A}R and nAChR agonists

	Residue	Efficacy±SEM (%)[a]
	nAChR W149	
norACh	Trp	81.8 ± 6.1
β,γ L9'S	F-Trp	96.0 ± 3.3
	F_2-Trp	69.2 ± 31
	F_3-Trp	40.4 ± 11
TMA	Trp	97.5 ± 5.1
β,γ L9'S	F-Trp	62.1 ± 38
	F_2-Trp	94.4 ± 4.7
	F_3-Trp	95.2 ± 3.3
Nicotine	Trp	88.9 ± 7.5
β,γ L9'S	F-Trp	81.8 ± 11
	F_2-Trp	82.8 ± 12
	F_3-Trp	67.7 ± 13
MeNicotinium	Trp	86.4 ± 7.5
β,γ L9'S	F-Trp	83.8 ± 9.8
	F_2-Trp	87.9 ± 2.8
	F_3-Trp	79.3 ± 11
	5-HT_{3A}R W183	
N-Me-5-HT	Trp	70.7 ± 1.6
	F-Trp	78.5 ± 3.3
	F_2-Trp	70.3 ± 2.5
	F_3-Trp	71.8 ± 3.4
5-HTQ	Trp	75.0 ± 1.7
	F-Trp	70.0 ± 7.1
	F_2-Trp	70.3 ± 11
	F_3-Trp	91.8 ± 4.3

a efficacy is reported as the relative percentage of I_{max} for a given agonist to I_{max} of ACh or 5-HT

2.3 Discussion

The agonist response of a ligand-gated ion channel testifies to the organizing power of weak, non-covalent interactions. As the neurotransmitter approaches the much larger receptor, it must not be lured in by sites whose charge, shape, and hydrophobicity resemble the intended binding site. Instead, the molecule diffuses within the synaptic cleft and is drawn exactly to the appropriate location to trigger channel opening. In the case of the nicotinic acetylcholine receptor, we have previously proposed a unique role for Trp149 in the α subunit in the binding of the natural agonist, acetylcholine.[8] Based on subtle alterations of the electrostatic surface of the side chain at this position, it was concluded that this site participates in a strong cation-π interaction with the quaternary ammonium center of ACh. More recent structural work from other labs on AChBP has confirmed this conclusion.[2] The work presented here extends this technique to the serotonin receptor, 5-HT_{3A}R. In addition, the experimental scope is expanded at both the nAChR and 5-HT_{3A}R to consider in greater detail the nature of the interaction between agonist and receptor. Homology between the 5-HT_{3A}R, the alpha subunit of the muscle nAChR, and AChBP is significant, with strong conservation of the tryptophan residues making up two sides of the ligand-binding site box. In addition, two of the three tyrosine residues seen in the nAChR and AChBP are aromatic amino acids in 5-HT_{3A}R (Figure 2.2).[32]

The introduction of a series of fluorinated Trp analogs at position 183 of the mouse 5-HT_{3A}R provides clear evidence for a cation-π interaction between this residue and serotonin, as suggested by earlier site-directed mutagenesis studies.[33] This interaction appears to be unique to Trp183. Substitution of the fluorinated Trp series at

Trp 90— also in the binding site region— causes no significant effects. We thus conclude that both the nAChR and the 5-HT_{3A}R make use of a single potent cation-π interaction in recognizing the ammonium centers of their respective agonists.

Interestingly, the slope of the plot relating EC_{50} to calculated cation-π binding energy (the fluorination plot) is visibly different for ACh binding to nAChR than serotonin binding to the 5-HT_{3A}R. Inspection of Figure 2.5c shows that the serotonin slope is markedly steeper. We interpret this to mean that the strength of the cation-π interaction between the agonist and the relevant tryptophan is greater when serotonin is the agonist than when ACh is the agonist. This result is consistent with expectations based on electrostatics.[34] As shown in Figure 2.4, the smaller, primary ammonium center of serotonin presents a more focused positive charge than the quaternary center of ACh. Given the strong electrostatic component of the cation-π interaction, smaller ions are expected to show a stronger interaction.

The data for ACh and serotonin also provide one way to address a long-standing issue in molecular recognition: what is the strength of a cation-π interaction? From Figure 2.3a, it may be observed that the surface of F_4-Trp is essentially electrostatically neutral. Thus, a comparison of F_4-Trp and Trp provides a measure of the *electrostatic component* of the cation-π interaction. The F_4-Trp/Trp ratio reflects the energy cost of removing the attractive electrostatics, but maintaining the residue as if the Trp were replaced by a hydrophobic residue of the same shape. This new residue maintains most van der Waals and dispersion interactions, but cannot experience a cation-π interaction. For ACh, the F_4-Trp/Trp ratio is 54. For serotonin, the F_4-Trp EC_{50} value is obtained by extrapolation of the line in Figure 2.5c which leads to a F_4-Trp/Trp ratio of 836. If these

are viewed as ratios of binding constants, then the implied energetics of a cation-π interaction are 2.4 kcal/mol and 4.0 kcal/mol, respectively for ACh and serotonin. These are consistent with other estimates of the magnitude of the cation-π interaction,[7] and further establish that this non-covalent binding force is comparable to, or stronger than, any other individual force considered in biological recognition.

In an effort to probe the molecular recognition properties of these receptors further, we studied the effects of varying the alkylation state of the cationic center of the agonist. In such studies, a clear distinction emerges between the 5-HT_{3A}R and the nAChR. At the serotonin receptor, the monoalkylated agonist, N-Me-5-HT and the quaternary agonist, 5-HTQ show essentially the same EC_{50} as the natural agonist 5-HT. This suggests that the 5-HT_{3A}R agonist binding site is fairly tolerant, accommodating the much bulkier 5-HTQ with no loss in potency. These two unnatural agonists respond to fluorination much like the natural agonist, serotonin, although the perfect linear trend of Figure 2.5c is not reproduced. We hesitate to provide an extensive interpretation of this subtle distinction in which multiple variables, including both the agonist and the protein, are being changed. However, it is clear that a strong cation-π interaction to Trp 183 is involved with all of these agonists.

The nAChR behaves quite differently from the 5-HT_{3A}R in this regard. First, the change from ACh to norACh leads to a very large increase in EC_{50}. Simply removing one methyl group from ACh produces a very low-potency agonist. In fact, norACh is comparable in potency to tetramethylammonium (TMA), which lacks several moieties of the ACh molecule. Interestingly, the quaternary TMA— although a very low-potency agonist— does show a fluorination trend that is similar to that of ACh (Figure 2.7). The

norACh fluorination trend is less well-behaved with a large increase for F-Trp, followed by minimal further effects for F_2-Trp and F_3-Trp, which are then followed by a downturn at F_4-Trp (Figure 2.7). While this suggests some kind of cation-π interaction for the norACh agonist, more subtle factors may also be operative for this low-potency, non-native agonist. Clearly, the nAChR is much more sensitive to alterations in the region of Trp α149 than the 5-HT_{3A}R is to comparable changes with the aligned Trp 183.

This leaves the case of nicotine— an obviously important agonist of the nAChR. Before discussing the results, a few general comments are in order. The receptor studied here is the muscle-type receptor— the isoform found at the neuromuscular junction in the peripheral nervous system. Nicotine is a full agonist at this receptor, but as shown in Table 2.2, nicotine is not an especially potent agonist at the muscle receptor. The behavioral and addictive effects of nicotine arise exclusively from effects on the *neuronal* nAChRs.[35-38] These receptors are expressed widely in the central nervous system.[39, 40] While the overall architecture of neuronal nAChR is no doubt the same as the muscle type described here, the neuronal receptors are comprised of different combinations of α and β (non-α) subunits. There are many variants of each subunit, but they are highly homologous to the muscle subunits, and all the residues discussed here are conserved in the neuronal receptors. At present, at least 10 α and 4 β forms are known, termed $\alpha_{1\text{-}10}$ and $\beta_{1\text{-}4}$ (α_1 and β_1 are the muscle forms; all the rest are neuronal). Nicotine addiction is thought to depend partially on receptors formed from α_4 and β_2 subunits (stoichiometry unknown) and perhaps receptors involving α_7.[37, 38, 41, 42] While we believe our findings are clearly relevant to the pharmacology of nicotine, it must be remembered that subtle variations could arise in comparable studies of the neuronal receptors.

The fluorination plot for nicotine is shown in Figure 2.8b. In light of our findings for ACh versus norACh, we also studied N-Me-nicotinium in which the pyrrolidine nitrogen has been quaternarized. Interestingly, these two nicotinoid agonists are similar, both in potency and in their fluorination plots. The nicotine fluorination plot has the shallowest slope of any agonist examined at either the nAChR or the 5-HT_{3A}R. After a relatively small jump in EC_{50} for F-Trp, only very small changes in EC_{50} are seen upon further fluorination of Trp α149. This is strong evidence that nicotine does not make a strong cation-π interaction with Trp α149 of the muscle-type nAChR.

One possibility is that nicotine makes a cation-π interaction with one of the other aromatics that form the "aromatic box" of the nAChR binding site. A sensible candidate is γ55/δ57— the other conserved Trp in the agonist binding site. This residue has been implicated in nicotine binding by photoaffinity labeling studies from the Cohen group.[43, 44] As a probe of this site, we studied the pair 5-CN-Trp/5-Br-Trp. It has been previously shown that this nearly isosteric pair can provide a good qualitative indication of a cation-π interaction, since the cyano group is much more strongly deactivating than the bromo. The pair differ by a factor of 57 for ACh at Trp α149.[8] However, no significant effect is seen at γ55/δ57 with nicotine (or ACh) as the agonist, ruling out this site for a cation-π interaction with nicotine at the muscle receptor.

Subsequent to the completion of this work, several studies examining the anomalous binding properties of nicotine were reported. Taken together, these studies provide a more detailed portrait of nicotine binding to the nAChR. Modeling studies based on the structure of AChBP suggested a hydrogen bonding interaction from the N^+–H of nicotine to the backbone carbonyl of Trp α149.[45, 46] Amanda Cashin and E.

James Petersson, in a study combining both functional data from backbone ester mutations at Thr α150 and computational work, demonstrated that nicotine binding depends on a hydrogen bond with the backbone carbonyl of α149.[47] More recently Sixma and co-workers reported the crystal structure of AChBP in the presence of bound nicotine.[5] This structure verified that nicotine does not form a cation-π interaction with Trp α149, and that bound nicotine does indeed make a hydrogen bond with the backbone carbonyl of α149.

The conclusion that nicotine does not bind to the muscle nAChR via a cation-π interaction with tryptophan residues in the aromatic box has implications for existing pharmacophore models of the nAChR. All current pharmacophore models align the quaternary ammonium of ACh with the protonated tertiary amine of nicotine.[25-29] It seems an unavoidable conclusion that such a model requires a cation-π interaction between the cationic center of nicotine and Trp α149, but it is now clear that, at least in the muscle nAChR, such a cation-π interaction does not exist. The data with norACh suggest that the nAChR is quite sensitive to variations in agonist structure at the cationic center— much more so than the 5-HT_{3A}R. As nicotine analogs are assuming a greater prominence for drug leads in a variety of important diseases, some caution in applying the standard pharmacophore model seems to be in order.

2.4 Conclusions

Earlier work in the Dougherty group demonstrated that the nonsense suppression methodology provides a powerful tool for evaluating drug-receptor interactions. In particular, fluorination plots can clearly identify a specific cation-π interaction between an agonist and its receptor. Here, we build upon those findings in several ways.

A clear cation-π interaction between serotonin and Trp 183 of the 5-HT_{3A}R is established. A measure of the magnitude of the electrostatic component of the cation-π interaction is provided. We find it to be worth ~2 kcal/mol for ACh at the nAChR and ~4 kcal/mol for serotonin at the 5-HT_{3A}R. Studies of other agonists highlight the differences between the two homologous receptors: the nAChR and the 5-HT_{3A}R. The latter is relatively tolerant of changes at the cationic center and maintains a cation-π interaction, while the nAChR seems quite sensitive to changes in the nature of the cationic center of the agonist. Finally, studies of the binding of nicotine to the muscle nAChR suggest that present pharmacophore models require revision. Work on the neuronal nAChR will be required to further explore this issue.

2.5 Methods

2.5.1 Electrophysiology

Stage VI oocytes of *Xenopus laevis* were harvested according to approved procedures. Recordings were made 24 to 72 hours post-injection in standard two-electrode voltage clamp mode. Oocytes were superfused with calcium-free ND96 solution, as previously reported[8]. Nicotinic agonists were either synthesized as described earlier (N-methyl-nicotinium)[48], or purchased from Sigma/Adrich/RBI ([-]-nicotine tartrate) or Acros Organics (the tertiary ACh analog, 2-dimethyl aminoethyl acetate). Serotonin and its analogs were purchased from Sigma/Adrich/RBI. All drugs were prepared in sterile ddi water for dilution into calcium-free ND96. Dose-response data were obtained for a minimum of eight concentrations of agonists for a minimum of three

different cells. Curves were fit to the Hill equation to determine EC_{50} and Hill coefficient.

2.5.2 Unnatural amino acid suppression

Synthetic amino acids were conjugated to the dinucleotide dCA and ligated to truncated 74 nt tRNA as described.[9] Deprotection of charged tRNA was carried out by photolysis immediately prior to co-injection with mRNA in the manner described.[8, 49] Typically, 25 ng tRNA were injected per oocyte along with mRNA in a total volume of 50 nL per cell. mRNA was prepared by *in vitro* runoff transcription using the Ambion mMagic mMessage kit. Mutation to insert the *amber* stop codon at the site of interest was carried out by standard means and was verified by sequencing through both strands. For nAChR suppression, a total of 4.0 ng of mRNA was injected in the subunit ratio of 10:1:1:1 α:β:γ:δ. In many cases, one or more subunits contained a L9'S mutation, as discussed above. As reported previously, mouse muscle embryonic nAChR in the pAMV vector was used. For suppression in homomeric 5-HT_{3A}R, 5.0 ng of mRNA was injected. Mouse 5-HT_{3A}R was used in all cases, in the pAMV vector. Negative and positive controls for suppression were performed in the following way: as a negative control, truncated 74 nt tRNA or truncated tRNA ligated to dCA was co-injected with mRNA in the same manner as fully charged tRNA. At the positions studied here, no current was ever observed from these negative controls. The positive control involved wild-type recovery by co-injection with 74 nt tRNA ligated to dCA-Trp. In all cases, the dose-response was indistinguishable from injection of wild-type mRNA alone.

2.6 References

1. Armstrong, N.; Gouaux, E., Mechanisms for activation and antagonism of an AMPA-sensitive glutamate receptor: crystal structures of the GluR2 ligand binding core. *Neuron* **2000,** 28, (1), 165-81.
2. Brejc, K.; van Dijk, W. J.; Klaassen, R. V.; Schuurmans, M.; van Der Oost, J.; Smit, A. B.; Sixma, T. K., Crystal structure of an ACh-binding protein reveals the ligand-binding domain of nicotinic receptors. *Nature* **2001,** 411, (6835), 269-76.
3. Mayer, M. L.; Olson, R.; Gouaux, E., Mechanisms for ligand binding to GluR0 ion channels: crystal structures of the glutamate and serine complexes and a closed apo state. *J Mol Biol* **2001,** 311, (4), 815-36.
4. Miyazawa, A.; Fujiyoshi, Y.; Stowell, M.; Unwin, N., Nicotinic acetylcholine receptor at 4.6 A resolution: transverse tunnels in the channel wall. *J Mol Biol* **1999,** 288, (4), 765-86.
5. Celie, P. H. N.; van Rossum-Fikkert, S. E.; van Dijk, W. J.; Brejc, K.; Smit, A. B.; Sixma, T. K., Nicotine and carbamylcholine binding to nicotinic acetylcholine receptors as studied in AChBP crystal structures. *Neuron* **2004,** 41, (6), 907-914.
6. Dougherty, D. A., Cation-pi interactions in chemistry and biology: A new view of benzene, Phe, Tyr, and Trp. *Science* **1996,** 271, (5246), 163-168.
7. Ma, J. C.; Dougherty, D. A., The cation-pi interaction. *Chemical Reviews* **1997,** 97, (5), 1303-1324.
8. Zhong, W. G.; Gallivan, J. P.; Zhang, Y. N.; Li, L. T.; Lester, H. A.; Dougherty, D. A., From ab initio quantum mechanics to molecular neurobiology: A cation-pi binding site in the nicotinic receptor. *Proceedings of the National Academy of Sciences of the United States of America* **1998,** 95, (21), 12088-12093.
9. Nowak, M. W.; Gallivan, J. P.; Silverman, S. K.; Labarca, C. G.; Dougherty, D. A.; Lester, H. A., In vivo incorporation of unnatural amino acids into ion channels in Xenopus oocyte expression system. *Methods in Enzymology* **1998,** 293, 504-529.
10. Thorson, J. S.; Cornish, V. W.; J.E., B.; S.T., C.; Yano, T.; Schultz, P. G., A biosynthetic approach for the incorporation of unatural amino acids into proteins. *Topics in Current Chemistry* **1998,** 77, 43-73.
11. Gilmore, M. A.; Steward, L. E.; Chamberlin, A. R., Incorporation of noncoded amino acids by in vitro protein biosynthesis. *Topics in Current Chemistry* **1999,** 202, 77-99.
12. Sisido, M.; Hohsaka, T., Extension of protein functions by the incorporation of nonnatural amino acids. *Bulletin of the Chemical Society of Japan* **1999,** 72, (7), 1409-1425.
13. Mecozzi, S.; West, A. P.; Dougherty, D. A., Cation-pi interactions in simple aromatics: Electrostatics provide a predictive tool. *Journal of the American Chemical Society* **1996,** 118, (9), 2307-2308.
14. Mecozzi, S.; West, A. P.; Dougherty, D. A., Cation-pi interactions in aromatics of biological and medicinal interest: Electrostatic potential surfaces as a useful qualitative guide. *Proceedings of the National Academy of Sciences of the United States of America* **1996,** 93, (20), 10566-10571.

15. Labarca, C.; Nowak, M. W.; Zhang, H.; Tang, L.; Deshpande, P.; Lester, H. A., Channel gating governed symmetrically by conserved leucine residues in the M2 domain of nicotinic receptors. *Nature* **1995,** 376, (6540), 514-6.
16. Kearney, P. C.; Nowak, M. W.; Zhong, W.; Silverman, S. K.; Lester, H. A.; Dougherty, D. A., Dose-response relations for unnatural amino acids at the agonist binding site of the nicotinic acetylcholine receptor: tests with novel side chains and with several agonists. *Mol Pharmacol* **1996,** 50, (5), 1401-12.
17. Kenakin, T., Efficacy in drug receptor theory: outdated concept or under-valued tool? *Trends Pharmacol Sci* **1999,** 20, (10), 400-5.
18. Maricq, A. V.; Peterson, A. S.; Brake, A. J.; Myers, R. M.; Julius, D., Primary structure and functional expression of the 5HT3 receptor, a serotonin-gated ion channel. *Science* **1991,** 254, (5030), 432-7.
19. Davies, P. A.; Pistis, M.; Hanna, M. C.; Peters, J. A.; Lambert, J. J.; Hales, T. G.; Kirkness, E. F., The 5-HT3B subunit is a major determinant of serotonin-receptor function. *Nature* **1999,** 397, (6717), 359-63.
20. Brady, C. A.; Stanford, I. M.; Ali, I.; Lin, L.; Williams, J. M.; Dubin, A. E.; Hope, A. G.; Barnes, N. M., Pharmacological comparison of human homomeric 5-HT3A receptors versus heteromeric 5-HT3A/3B receptors. *Neuropharmacology* **2001,** 41, (2), 282-4.
21. Bhattacharya, A.; Dang, H.; Zhu, Q. M.; Schnegelsberg, B.; Rozengurt, N.; Cain, G.; Prantil, R.; Vorp, D. A.; Guy, N.; Julius, D.; Ford, A.; Lester, H. A.; Cockayne, D. A., Uropathic observations in mice expressing a constitutively active point mutation in the 5-HT3A receptor subunit. *Journal of Neuroscience* **2004,** 24, (24), 5537-5548.
22. Dang, H.; England, P. M.; Farivar, S. S.; Dougherty, D. A.; Lester, H. A., Probing the role of a conserved M1 proline residue in 5-hydroxytryptamine(3) receptor gating. *Molecular Pharmacology* **2000,** 57, (6), 1114-1122.
23. Abraham, M. H.; Grellier, P. L.; Prior, D. V.; Duce, P. P.; Morris, J. J.; Taylor, P. J., Hydrogen-Bonding .7. A Scale of Solute Hydrogen-Bond Acidity Based on Log K-Values for Complexation in Tetrachloromethane. *Journal of the Chemical Society-Perkin Transactions 2* **1989**, (6), 699-711.
24. Smart, B. E., Fluorine substituent effects (on bioactivity). *Journal of Fluorine Chemistry* **2001,** 109, (1), 3-11.
25. Tonder, J. E.; Olesen, P. H., Agonists at the alpha4beta2 nicotinic acetylcholine receptors: structure-activity relationships and molecular modelling. *Curr Med Chem* **2001,** 8, (6), 651-74.
26. Schmitt, J. D., Exploring the nature of molecular recognition in nicotinic acetylcholine receptors. *Curr Med Chem* **2000,** 7, (8), 749-800.
27. Tonder, J. E.; Hansen, J. B.; Begtrup, M.; Pettersson, I.; Rimvall, K.; Christensen, B.; Ehrbar, U.; Olesen, P. H., Improving the nicotinic pharmacophore with a series of (Isoxazole)methylene-1-azacyclic compounds: synthesis, structure-activity relationship, and molecular modeling. *J Med Chem* **1999,** 42, (24), 4970-80.
28. Sheridan, R. P.; Nilakantan, R.; Dixon, J. S.; Venkataraghavan, R., The ensemble approach to distance geometry: application to the nicotinic pharmacophore. *J Med Chem* **1986,** 29, (6), 899-906.
29. Curtis, L.; Chiodini, F.; Spang, J. E.; Bertrand, S.; Patt, J. T.; Westera, G.; Bertrand, D., A new look at the neuronal nicotinic acetylcholine receptor pharmacophore. *Eur J Pharmacol* **2000,** 393, (1-3), 155-63.

30. Kenakin, T., Inverse, protean, and ligand-selective agonism: matters of receptor conformation. *Faseb J* **2001,** 15, (3), 598-611.
31. Colquhoun, D., Binding, gating, affinity and efficacy: the interpretation of structure-activity relationships for agonists and of the effects of mutating receptors. *Br J Pharmacol* **1998,** 125, (5), 924-47.
32. Boess, F. G.; Steward, L. J.; Steele, J. A.; Liu, D.; Reid, J.; Glencorse, T. A.; Martin, I. L., Analysis of the ligand binding site of the 5-HT3 receptor using site directed mutagenesis: importance of glutamate 106. *Neuropharmacology* **1997,** 36, (4-5), 637-47.
33. Spier, A. D.; Lummis, S. C., The role of tryptophan residues in the 5-Hydroxytryptamine(3) receptor ligand binding domain. *J Biol Chem* **2000,** 275, (8), 5620-5.
34. Schmitt, J. D.; Sharples, C. G.; Caldwell, W. S., Molecular recognition in nicotinic acetylcholine receptors: the importance of pi-cation interactions. *J Med Chem* **1999,** 42, (16), 3066-74.
35. Benowitz, N. L., Pharmacology of nicotine: addiction and therapeutics. *Annu Rev Pharmacol Toxicol* **1996,** 36, 597-613.
36. Dani, J. A.; Heinemann, S., Molecular and cellular aspects of nicotine abuse. *Neuron* **1996,** 16, (5), 905-8.
37. Picciotto, M. R.; Zoli, M.; Rimondini, R.; Lena, C.; Marubio, L. M.; Pich, E. M.; Fuxe, K.; Changeux, J. P., Acetylcholine receptors containing the beta2 subunit are involved in the reinforcing properties of nicotine. *Nature* **1998,** 391, (6663), 173-7.
38. Tapper, A. R.; McKinney, S. L.; Nashmi, R.; Schwarz, J.; Deshpande, P.; Labarca, C.; Whiteaker, P.; Marks, M. J.; Collins, A. C.; Lester, H. A., Nicotine activation of alpha 4*receptors: Sufficient for reward, tolerance, and sensitization. *Science* **2004,** 306, (5698), 1029-1032.
39. McGehee, D. S.; Role, L. W., Physiological diversity of nicotinic acetylcholine receptors expressed by vertebrate neurons. *Annu Rev Physiol* **1995,** 57, 521-46.
40. Jones, S.; Sudweeks, S.; Yakel, J. L., Nicotinic receptors in the brain: correlating physiology with function. *Trends Neurosci* **1999,** 22, (12), 555-61.
41. Lena, C.; Changeux, J. P., Pathological mutations of nicotinic receptors and nicotine-based therapies for brain disorders. *Curr Opin Neurobiol* **1997,** 7, (5), 674-82.
42. Marubio, L. M.; del Mar Arroyo-Jimenez, M.; Cordero-Erausquin, M.; Lena, C.; Le Novere, N.; de Kerchove d'Exaerde, A.; Huchet, M.; Damaj, M. I.; Changeux, J. P., Reduced antinociception in mice lacking neuronal nicotinic receptor subunits. *Nature* **1999,** 398, (6730), 805-10.
43. Xie, Y.; Cohen, J. B., Contributions of Torpedo nicotinic acetylcholine receptor gamma Trp-55 and delta Trp-57 to agonist and competitive antagonist function. *J Biol Chem* **2001,** 276, (4), 2417-26.
44. Chiara, D. C.; Middleton, R. E.; Cohen, J. B., Identification of tryptophan 55 as the primary site of [3H]nicotine photoincorporation in the gamma-subunit of the Torpedo nicotinic acetylcholine receptor. *FEBS Lett* **1998,** 423, (2), 223-6.
45. Schapira, M.; Abagyan, R.; Totrov, M., Structural model of nicotinic acetylcholine receptor isotypes bound to acetylcholine and nicotine. *BMC Struct. Biol.* **2002,** 2, (1), 1.
46. Le Novere, N.; Grutter, T.; Changeux, J. P., Models of the extracellular domain of the nicotinic receptors and of agonist- and Ca2+-binding sites. *Proc. Natl. Acad. Sci. USA* **2002,** 99, (5), 3210-3215.

47. Cashin, A. L., Petersson, E.J., Lester, H.A., and Dougherty, D.A., *Journal of the American Chemical Society* **2004,** in press.
48. Seeman, J. I.; Whidby, J. F., The iodomethylation of nicotine. An unusual example of competitive nitrogen alkylation. *J Org Chem* **1976,** 41, (24), 3824-6.
49. Li, L. T.; Zhong, W. G.; Zacharias, N.; Gibbs, C.; Lester, H. A.; Dougherty, D. A., The tethered agonist approach to mapping ion channel proteins toward a structural model for the agonist binding site of the nicotinic acetylcholine receptor. *Chemistry & Biology* **2001,** 8, (1), 47-58.